Journal of Statistical Physics, Vol. 40, Nos. 1/2, 1985

Orientational Structure of Dipolar Hard Spheres near a Hard Neutral Wall

D. Levesque[1] **and J.-J. Weis**[1]

Received November 21, 1984

Spherical boundaries are used in a Monte Carlo simulation to calculate the angular structure of dipolar hard spheres near a neutral hard wall.

KEY WORDS: Surface structure; Monte Carlo simulation; dipolar hard sphere.

1. INTRODUCTION

In recent molecular dynamics simulations Bossis and coworkers$^{(1-4)}$ demonstrated the usefulness of using an isolated spherical sample to determine the bulk properties of dipolar systems. More specifically, their calculations show that for system sizes of the order of 1000–1500 particles (in three dimensions) a large inner region of the sample has constant density and exhibits macroscopic dielectric behavior thus allowing a reliable determination of the dielectric properties, both static and dynamic.$^{(1)}$

Analogously, Powles and coworkers determine the dielectric constant$^{(5)}$ and surface properties$^{(6,7)}$ of a microscopic drop of polar liquid in equilibrium in its own vapor.

In the present work a spherical volume simulation is applied to study the orientational structure of dipolar molecules near a hard wall. In this case the surface boundary is simply assumed to be impenetrable to the particles. Again a system size of 1000–1500 particles appears sufficient to obtain most of the surface properties independent of curvature even for

---

[1] Laboratoire de Physique Théorique et Hautes Energies (Laboratoire associé au Centre National de la Recherche Scientifique), Université de Paris-Sud, Bâtiment 211, 91405 Orsay, France.

0022-4715/85/0700-0029$04.50/0 © 1985 Plenum Publishing Corporation

fairly high dipole moments. At the same time the bulk properties can be determined.

For dipolar systems these boundaries seem vastly more convenient than the more traditional rectangular ones (two opposite faces acting as walls) to which the Ewald summation or the reaction field methods necessary to correct for the long-range dipolar interaction would be extremely time-consuming to apply.

In the Monte Carlo calculations which will be described in Section 2 we adopt the simple model of dipolar hard spheres near a hard neutral wall. In this model, the particles interact among themselves through the potential

$$\begin{aligned} v_{ij}(r_{ij}) &= +\infty, \qquad r_{ij} \leqslant \sigma \\ &= -\frac{\beta\mu^2}{r_{ij}^3}\,\Phi^{112}(ij), \qquad r_{ij} > \sigma \end{aligned} \tag{1}$$

and with the wall via the wall–particle interaction

$$v_{Wi}(r_i) = +\infty, \qquad r_i \geqslant R \tag{2}$$

In Eq. (1)

$$\Phi^{112}(ij) = \frac{3(\mathbf{s}_i \cdot \mathbf{r}_{ij})(\mathbf{s}_j \cdot \mathbf{r}_{ij})}{r_{ij}^2} - \mathbf{s}_i \cdot \mathbf{s}_j \tag{3}$$

and μ is the dipole moment, $kT = \beta^{-1}$ the temperature, $\mathbf{s}_i$ a unit vector in the direction of the ith dipole moment, $\mathbf{r}_{ij} = \mathbf{r}_j - \mathbf{r}_i$, $r_{ij} = |\mathbf{r}_{ij}|$ where the location of particle i, $\mathbf{r}_i$, is measured from the center of the simulation sphere of radius R.

The main aim of our work is to determine the variations of the density profile from a nonpolar to a highly polar hard sphere system. These results, including bulk properties, are given in Section 3. Our main conclusions will be summarized in Section 4.

2. COMPUTER SIMULATIONS

Monte Carlo calculations were carried out for a system of $N = 1061$ dipolar hard spheres the centers of which were constrained to a spherical volume S with radius R such that the average density was

$$\rho_{\text{av}}\sigma^3 = \frac{N\sigma^3}{(4\pi/3)\,R^3} = 0.8$$

The dipole moments $\mu^{*2} = \mu^2/\sigma^3 kT$ ranged from 0 (pure hard spheres) to 3. For the highest dipole moment ($\mu^{*2} = 3$) a somewhat larger system was considered as well to detect possible curvature effects. For each case a total of 5.7 million configurations was generated after equilibrium. [The calculations were performed on the Cray-1 at École Polytechnique (Palaiseau).]

3. RESULTS

3.1. "Bulk" Properties

Reliable surface properties can only be obtained if the central region of the system behaves as an homogeneous bulk system. As a check we calculated the potential energy, pair correlation function, and dielectric constant in the inner region of the simulation sphere. More precisely, we define a "bulk" energy $\beta\bar{U}$ as the average energy of a particle belonging to the sphere S_0 concentric to S and having radius $R_0 = 0.4R$, i.e.,

$$\beta\bar{U} = \left\langle \sum_{\substack{i \neq j \\ i \in S_0, j \in S}} \beta v_{ij} \right\rangle \tag{4}$$

The projections $g^{000}(r_{ij})$, $h^{110}(r_{ij})$, and $h^{112}(r_{ij})$ of the pair distribution function $g(r_{ij}, \Omega_i, \Omega_j)$ on the rotational invariants $\Phi^{000} = 1$, $\Phi^{110} = \mathbf{s}_i \cdot \mathbf{s}_j$, and Φ^{112} given by (3) were evaluated for all pairs of particles (ij) such that $i \in S_0$, $j \in S$, and $|\mathbf{r}_j - \mathbf{r}_i| \leqslant R_0$.

Finally, the dielectric constant was estimated from the mean square dipole moment

$$g = \left\langle \frac{\left(\sum_{j \in S_i(R_0)} \boldsymbol{\mu}_j\right)^2}{N_i(R_0)} \right\rangle \tag{5}$$

through use of the relation$^{(1)}$

$$\frac{(\varepsilon - 1)[(\varepsilon + 2)(2\varepsilon + 1) - 2(R_0/R)^3(\varepsilon - 1)^2]}{9\varepsilon(\varepsilon + 2)} = yg \tag{6}$$

where

$$y = \frac{4\pi\rho\beta\mu^2}{9} \tag{7}$$

In (5) $S_i(R_0)$ denotes a sphere of radius R_0 centered at particle $i \in S_0$ and $N_i(R_0)$ the number of particles inside this sphere. Equation (6) applies, strictly speaking, only to a spherical sample centered at the origin and not to the decentered ones used in Eq. (5). Correction terms have been evaluated by a method analogous to that described by Bossis(2) for two-dimensional systems, but, as they turn out to be smaller than the statistical error in our calculations, have been neglected for the present purposes.

To decide whether the results obtained in the "bulk" region S_0 are those of a homogeneous system we compare them with QHNC integral equation(8) results. For the bulk density considered ($\rho_0\sigma^3 = 0.7$, see below) and dipole moments $\mu^{*2} \lesssim 2$ these are sufficiently accurate(9) that one can avoid performing "exact" calculations for an homogeneous system using, e.g., Ewald summation or reaction field methods.

The projections h^{110} and h^{112} are compared in Figs. 1 and 2 for $\rho_0\sigma^3 = 0.7$ and $\mu^{*2} = 2.0$. The agreement is excellent. The slight discrepancies in h^{110} merely reflect a (small) deficiency of the QHNC equations.(9)

The energies do compare favorably (cf. Table I); the dielectric constants, on the contrary, are not in good agreement. This result is, however, not surprising as it is now well known that the QHNC equation overestimates the dielectric constant.(1,9,10) Very recently, it has been shown(11) that for dipolar hard spheres the full solution of the HNC equation gives a better estimate of ε. The corresponding values are seen to be in much closer agreement with the value derived from (6).

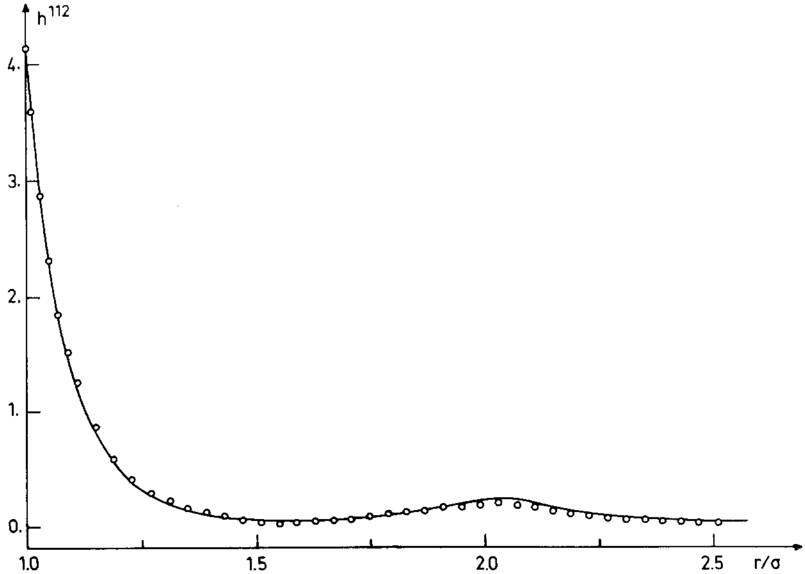

Fig. 1. Bulk correlation function $h^{112}(r)$ at $\rho_0\sigma^3 = 0.7$ and $\mu^{*2} = 2$. Solid line: QHNC equation; open circles: present Monte Carlo calculations (see text).

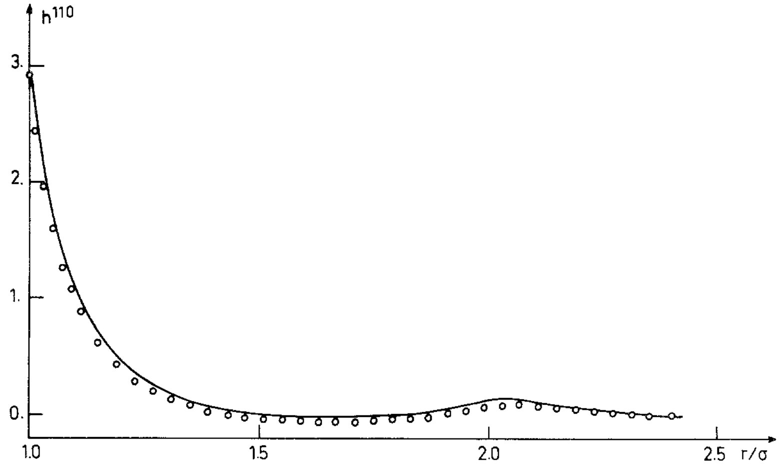

Fig. 2. Bulk correlation function h^{110} at $\rho_0\sigma^3=0.7$ and $\mu^{*2}=2$. Solid line: QHNC equation; open circles: present Monte Carlo calculations (see text).

3.2. Surface Properties

3.2.1. Density Profile. The density profiles defined by

$$\rho(r)=\left\langle \sum_i \delta(\mathbf{r}-\mathbf{r}_i)\right\rangle \tag{8}$$

are shown in Fig. 3 for $\mu^{*2}=0$, 1, 2, and 3. With increasing dipole moment the main changes occur in the immediate vicinity of the wall. The contact value decreases as a result of the lowering of the bulk pressure in accord with the exact relation

$$\rho(0)=\beta p_0 \tag{9}$$

The latter relation is satisfied to a fair degree of precision (cf. Table I) taking into account the combined statistical uncertainties on both the contact value and the "bulk" pressure calculated in S_0 by use of the relation

$$\beta p_0=\rho_0\left[1+\frac{2\pi}{3}\rho_0 g^{000}(\sigma)+\beta\bar{U}\right] \tag{10}$$

The subsequent layering which extends over a region of 3σ reflects mainly packing effects. A small shift away from the wall occurs in the positions of the first minimum and second maximum at the highest dipole moment accompanied by a small reduction of the amplitude of the oscillations. In all cases the "bulk" density is $\rho_0\sigma^3\simeq 0.7$.

Table I. Internal Energy, Density at Contact, and "Bulk" Properties as a Function of Dipole Moment ($\rho_0\sigma^3 = 0.7$)

			$\beta p_0\sigma^3$		$\beta\bar{U}$	$\beta U_0/N$	$g^{000}(\sigma)$		ε	
μ^{*2}	$\beta U/N$	$\rho(0)\,\sigma^3$	MC	QHNC	MC	QHNC	MC	QHNC	MC	QHNC
0	0	4.0 ± 0.15	3.92 $(3.997)^a$		0		3.14			
1	−0.825	3.8 ± 0.15	3.55	3.57	−0.877	−0.889	3.37	3.40	6.3	7.38 $(6.66)^b$
2	−2.371	3.20 ± 0.10	3.01	3.01	−2.48	−2.51	3.94	3.87	16	25.5 $(20)^b$
3	−4.24 -4.31^c	2.76 ± 0.10 2.78 ± 0.10^c	2.74 2.61^c	2.25 —	−4.35 -4.42^c	−4.44 —	4.96 4.88^c	4.54	28 31^c	80 $(49)^b$

[a] From Carnahan–Starling expression.(20)

[b] HNC.(21)

[c] Results for system of $N = 1505$ particles.

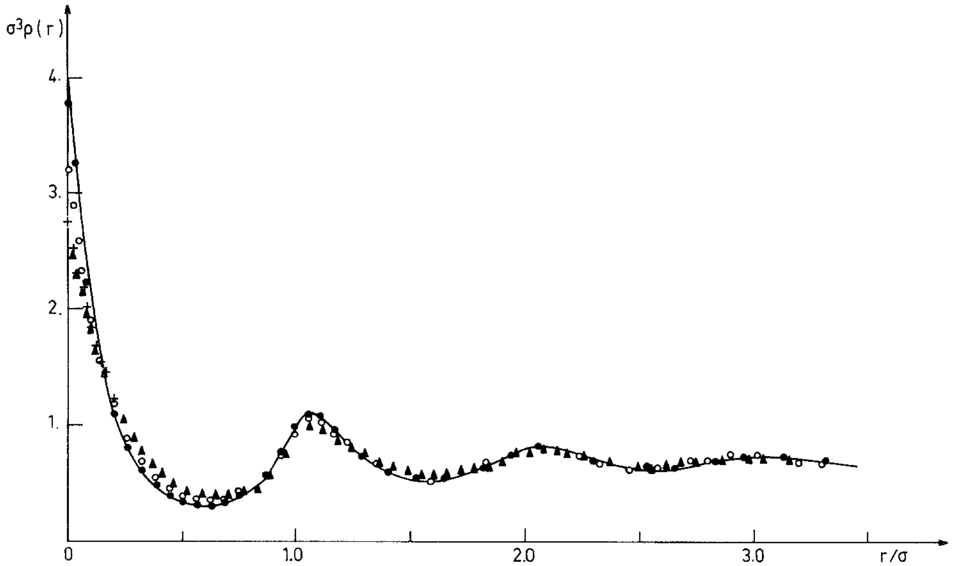

Fig. 3. Density profile at $\rho_0\sigma^3 = 0.7$ as a function of dipole moment. Solid line: pure hard spheres; solid circles: $\mu^{*2} = 1$; open circles: $\mu^{*2} = 2$; triangles: $\mu^{*2} = 3$ for system of 1061 particles and crosses for systems of 1505 particles (for $r > 0.5\sigma$ the profiles are identical in the statistical uncertainties).

It is noteworthy that the pure hard sphere density profile is in excellent agreement with previous ones(12,13) using a rectangular simulation cell and periodic boundary conditions in the directions parallel to the wall.[2] This result gives strong support for the adequacy of the present geometry.

3.2.2. Angular Density Profile. The orientational structure of the dipoles in the vicinity of the wall is obtained from the angle dependent one particle distribution function

$$\rho(r, \Omega) \equiv \rho(r, \theta) = \left\langle \sum_i \delta(\mathbf{r} - \mathbf{r}_i)\, \delta(\Omega - \Omega_i) \right\rangle \tag{11}$$

evaluated from a histogram of resolution $\Delta r = 0.08\sigma$ and $\Delta \cos\theta = 2/11$. In (11) θ denotes the angle between the dipole moment $\boldsymbol{\mu}$ and the direction of $\mathbf{r}$ (perpendicular to and pointing toward the wall). Figure 4 shows $\rho(r, \theta)/\rho_0$ for several fixed orientations of the dipole moment, whereas Fig. 5 shows $\rho(r, \theta)/\rho(r)$ as a function of $\cos\theta$ for increasing values of the distance from the wall. Statistics have been improved by averaging over the equally probable orientations θ and $\pi - \theta$.

---

[2] Unfortunately the authors of Ref. 13 do not give a graph of their density profile calculated at the density $\rho\sigma^3 \simeq 0.7$.

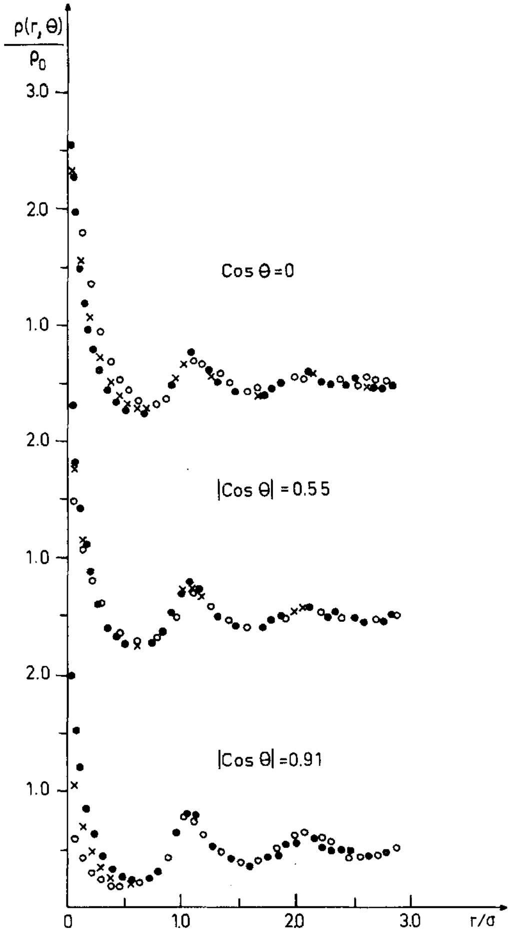

Fig. 4. Orientational density profile for fixed orientations of the dipole moment with respect to the direction normal to the wall. Solid circles: $\mu^{*2}=1$; open circles: $\mu^{*2}=2$; crosses: $\mu^{*2}=3$.

From these figures it is apparent that in the vicinity of the wall the dipoles show a clear preference, especially for high dipole moments, to align parallel to the wall in agreement with the conclusions reached for the waterlike models[14-18]; when one moves away from the wall the orientational order diminishes progressively. In the regions of the minima of the density oscillations a similar pattern subsists whereas near the maxima a very slight preference for orientations perpendicular to the wall occurs (cf. Fig. 5). This tendency is observed for all values of the dipole moment.

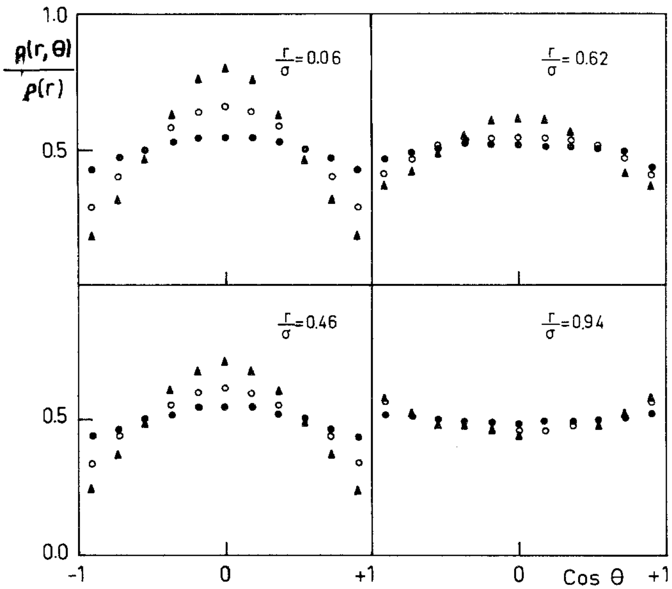

Fig. 5. Variation of the angular probability distribution function $\rho(r, \theta)/\rho(r)$ with distance from the wall. Solid circles: $\mu^{*2}=1$; open circles: $\mu^{*2}=2$; triangles: $\mu^{*2}=3$.

4. SUMMARY

The bulk and surface properties of a system of dipolar hard spheres confined by a spherical impenetrable neutral wall have been calculated by Monte Carlo. The density profile is mainly determined by steric effects except in the close vicinity of the wall where the dipole interactions pull the particles away from the wall as evidenced by the decrease of the contact value with increasing dipole moment. The preferential orientations of the dipoles in the layer adjacent to the wall and in the regions of the density minima is parallel to the wall. In the regions of the density maxima there is a slight preference for perpendicular orientations.

Varying the system size from 1000 to 1500 particles does not appreciably affect the density profile. The independence of the latter on curvature for systems larger than a thousand particles is further corroborated by the fact that for pure hard spheres it is undistinguishable from that obtained by using a rectangular simulation cell with periodic boundary conditions in the directions parallel to the walls.

Similar conclusions have been reached in a study by Thomson *et al.*(19) of the particle number dependence of the surface properties of Lennard-Jones drops. In this article it is established that the surface tension calculated with systems of $N \sim 1000$ particles are erroneous by 20%–50%. An estimation of $\beta\gamma\sigma^2$ can be obtained from the scaled particle theory(13,22) which gives $\beta\gamma\sigma^2 = -0.94$, -0.74, -0.48, and -0.37, respectively, for $\mu^{*2} = 0, 1, 2,$ and 3.

We conclude that the use of a spherical boundary is a convenient way to determine both the surface and bulk properties of polar systems, avoiding in particular the cumbersome Ewald summation method.

ACKNOWLEDGMENTS

We are grateful to P. Fries and G. N. Patey for supplying the HNC results of the dielectric constant.

REFERENCES

1. C. Hesse-Bezot, G. Bossis, and C. Brot, *J. Chem. Phys.* **80**:3399 (1984).
2. G. Bossis, B. Quentrec, and C. Brot, *Mol. Phys.* **39**:1233 (1980).
3. C. Brot, G. Bossis, and C. Hesse-Bezot, *Mol. Phys.* **40**:1053 (1980).
4. G. Bossis and C. Brot, *Mol. Phys.* **43**:1095 (1981).
5. J. G. Powles, R. F. Fowler, and W. A. B. Evans, *Chem. Phys. Lett.* **107**:280 (1984).
6. J. G. Powles, R. F. Fowler, and W. A. B. Evans, *Chem. Phys. Lett.* **96**:289 (1983).
7. J. G. Powles, R. F. Fowler, and W. A. B. Evans, *Phys. Lett.* **98A**:421 (1983).
8. G. N. Patey, *Mol. Phys.* **35**:1413 (1978).
9. G. N. Patey, D. Levesque, and J. J. Weis, *Mol. Phys.* **38**:219 (1979).
10. E. L. Pollock and B. J. Alder, *Physica* **101A**:275 (1980).
11. P. Fries and G. N. Patey, *J. Chem. Phys.* **82**:429 (1985).
12. B. Borštnik and A. Ažman, *Z. Naturforsch.* **33a**:1557 (1978).
13. J. R. Henderson and F. van Swol, *Mol. Phys.* **51**:991 (1984).
14. B. Jönsson, *Chem. Phys. Lett.* **82**:520 (1981).
15. M. Marchesi, *Chem. Phys. Lett.* **97**:224 (1983).
16. R. Sonnenschein and K. Heinziger, *Chem. Phys. Lett.* **102**:550 (1983).
17. G. Barabino, C. Gavotti, and M. Marchesi, *Chem. Phys. Lett.* **104**:478 (1984).
18. C. Y. Lee, J. A. McCammon, and P. J. Rossky, *J. Chem. Phys.* **80**:4448 (1984).
19. S. M. Thomson, K. E. Gubbins, J. P. R. B. Walton, R. A. R. Chantry, and J. S. Rowlinson, *J. Chem. Phys.* **81**:530 (1984).
20. N. F. Carnahan and K. E. Starling, *J. Chem. Phys.* **51**:635 (1969).
21. P. Fries and G. N. Patey, private communication.
22. H. Reiss, H. C. Frisch, E. Helfand, and J. L. Lebowitz, *J. Chem. Phys.* **32**:119 (1960).